Available online at www.sciencedirect.com
ScienceDirect
Sedimentary Geology 200 (2007) 347–361
Sedimentary Geology
www.elsevier.com/locate/sedgeo

A simple model for calculating tsunami flow speed from tsunami deposits

Bruce E. Jaffe [a,*], Guy Gelfenbuam [b]

[a] U.S. Geological Survey 400 Natural Bridges Dr., Santa Cruz, CA 95060, United States
[b] U.S. Geological Survey 345 Middlefield Rd., Menlo Park, CA 94025, United States

Abstract

This paper presents a simple model for tsunami sedimentation that can be applied to calculate tsunami flow speed from the thickness and grain size of a tsunami deposit (the inverse problem). For sandy tsunami deposits where grain size and thickness vary gradually in the direction of transport, tsunami sediment transport is modeled as a steady, spatially uniform process. The amount of sediment in suspension is assumed to be in equilibrium with the steady portion of the long period, slowing varying uprush portion of the tsunami. Spatial flow deceleration is assumed to be small and not to contribute significantly to the tsunami deposit. Tsunami deposits are formed from sediment settling from the water column when flow speeds on land go to zero everywhere at the time of maximum tsunami inundation. There is little erosion of the deposit by return flow because it is a slow flow and is concentrated in topographic lows. Variations in grain size of the deposit are found to have more effect on calculated tsunami flow speed than deposit thickness. The model is tested using field data collected at Arop, Papua New Guinea soon after the 1998 tsunami. Speed estimates of 14 m/s at 200 m inland from the shoreline compare favorably with those from a 1-D inundation model and from application of Bernoulli's principle to water levels on buildings left standing after the tsunami. As evidence that the model is applicable to some sandy tsunami deposits, the model reproduces the observed normal grading and vertical variation in sorting and skewness of a deposit formed by the 1998 tsunami.
Published by Elsevier B.V.

Keywords: Tsunami; Tsunami deposit; Sediment transport; Model; Hydrodynamics; Papua New Guinea

1. Introduction

In the past two decades, the study of tsunami deposits has increased rapidly (Dawson et al., 1988; Bourgeois et al., 1988; Peterson and Priest, 1995; Clague et al., 2000; Moore, 2000; Goff et al., 2000; Panegina et al., 2003; Williams et al., 2005; Peters et al., 2003). This research is fueled by the growing appreciation of the utility of tsunami deposits in tsunami risk assessment (Walsh et al., 2000; Jaffe and Gelfenbaum, 2002; Nanayama et al., 2003). Tsunami deposits are hard evidence that a tsunami inundated an area. Tsunami recurrence intervals can be estimated from dating a series of tsunami deposits (Hutchinson et al., 1997). Tsunami deposit research has focused on developing criteria for identifying tsunami deposits (Nanayama et al., 2000; Witter et al., 2001; Goff et al., 2004; Tuttle et al., 2004; Peters et al., 2003; Morton et al., this issue) and on improving the record of tsunamis for at risk regions (Kelsey et al., 2005). A small minority of these studies have capitalized on recent tsunami events to study modern tsunami deposits (Shi et al., 1995; Sato et al., 1995; Nishimura and Miyaji, 1995; Dawson et al., 1996;

* Corresponding author.
E-mail address: bjaffe@usgs.gov (B.E. Jaffe).

0037-0738/$ - see front matter. Published by Elsevier B.V.
doi:10.1016/j.sedgeo.2007.01.013

Minoura et al., 1997; Bourgeois et al., 1999; Gelfenbaum and Jaffe, 2003; Jaffe et al., 2003).

Studies of modern tsunami deposits have the advantage of being able to, at least qualitatively, relate characteristics of tsunamis (e.g.; runup, inundation, flow speed, flow depth) and deposit (e.g.; thickness, grain size, grading). Once these relations are learned, they can be applied to paleotsunami deposits to reconstruct paleotsunami characteristics.

This study exploits the common observation that many modern and paleo-sandy tsunami deposits are normally graded (Shi et al., 1995; Sato et al., 1995; Nishimura and Miyaji, 1995; Bourgeois et al., 1999; Gelfenbaum and Jaffe, 2003; Jaffe et al., 2003). An example of a normally graded tsunami deposit formed during the 1998 Papua New Guinea tsunami (Gelfenbaum and Jaffe, 2003) is shown in Fig. 1. Normally graded deposits typically form by settling of sediment from suspension. For sediment with the same density, particles with higher settling velocities (larger particles) preferentially reach the bed before those with lower settling velocities (smaller particles). It is reasonable to expect that many tsunami deposits form by settling from suspension.

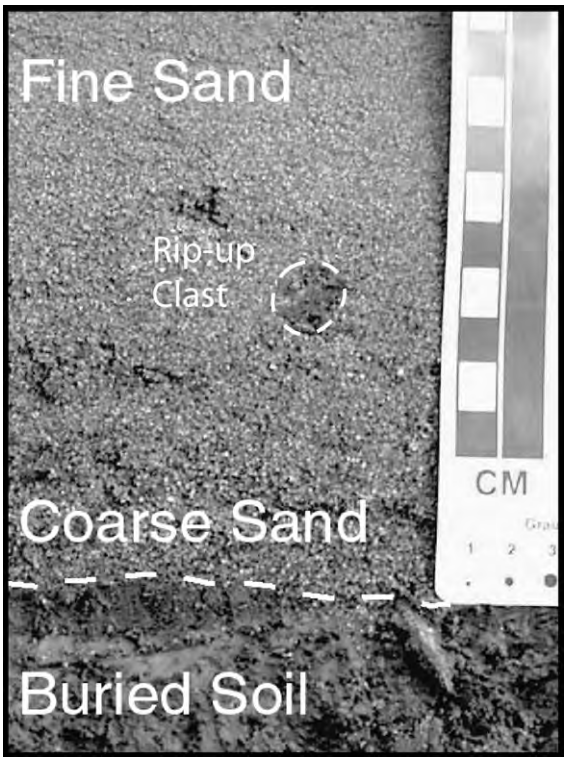

Fig. 1. Normally graded tsunami deposit at Arop, Papua New Guinea formed during the 1998 tsunami. Figure from Gelfenbaum and Jaffe (2003).

In this paper we present a simple model, which assumes that tsunami deposits form from sediment raining out from suspension, for calculating tsunami flow speed from the thickness and grain size distribution of a tsunami deposit.

2. Tsunami sedimentation

2.1. Conceptual model

Sediment transport during a tsunami may cause erosion or form a deposit. Erosion occurs when there is a spatial divergence in transport (more sediment leaving an area than coming in) or as the flow slows and sediment from the bed moves into the water column. A deposit is created by either a spatial convergence in transport (more coming into an area than leaving it) or as the flow wanes and sediment in the water column falls to the bed. Field investigations of modern tsunamis (Gelfenbaum and Jaffe, 2003; Jaffe et al., 2003, as well as investigations by the authors in Sri Lanka and Sumatra after the December 26, 2004 tsunami) observe three zones: (1) a zone of erosion extending from the shore inland, (2) a broad zone of tsunami deposition landward of the erosion zone, and (3) a narrow zone with neither deposition nor erosion near the limit of inundation. A conceptual model for the processes causing erosion and deposition in a tsunami is shown in Fig. 1. The zone of erosion is formed by the tsunami accelerating as it moves onshore, the broad zone of deposition is created by quasi-uniform flow where the tsunami is neither strongly accelerating nor decelerating and sediment settles out of suspension when flow speed drops to zero everywhere after tsunami flooding, and the narrow zone near the limit of inundation with neither erosion or deposition is created by the tsunami flow speed dropping to a point where it is not able to transport sediment. The width of each of these zones depends on tsunami characteristics, sediment supply, the substrate that the tsunami travels over, and topography. There are cases where not all three of the zones are present, but commonly they are (Gelfenbaum and Jaffe, 2003; Jaffe et al., 2003).

This conceptual model is most applicable to gentle sloping broad coastal plains. Under these conditions the zone of deposition is often broad and much of the tsunami deposit is not eroded by the return flow, which either is not flowing fast or is concentrated in topographic lows (Bourgeois et al., 1999; Gelfenbaum and Jaffe, 2003; Jaffe et al., 2003; field observations by the authors in Sumatra and Sri Lanka after the 26 December 2004 Indian Ocean Tsunami).

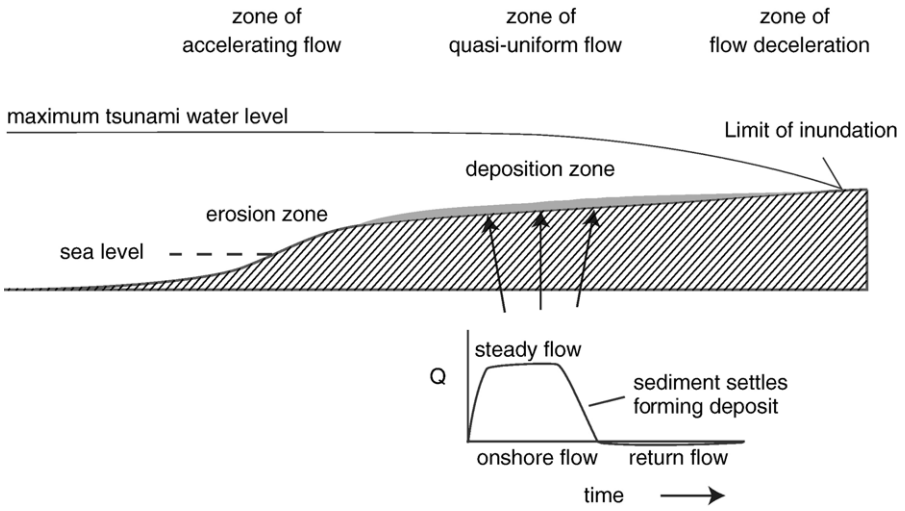

Fig. 2. Conceptual model of tsunami sedimentation. Deposit is formed in a zone of spatially quasi-uniform flow by sediment settling out of suspension when the tsunami flow speed goes to zero at the end of the onshore flow. Because the deposition zone is spatially quasi-uniform, the same temporal variation in flow speed applies to all locations in this zone. Quasi-uniform flow limits the amount of sediment deposited by sediment flux convergences, resulting in deposition from suspension being the primary process for tsunami deposit formation. The return flow is weak and concentrated in topographic lows and does not erode much of the deposit that formed during the onshore flow.

2.2. Modeling approach

Our approach is to quantify the conceptual model for the general case and, before solving the complete set of equations, simplify them using characteristics of tsunami flow and field observations of tsunami deposits. We solve this simplified model, explore the sensitivity of the model to poorly constrained input and model parameters, and evaluate where the simplifying assumptions are supported by field observations.

The full erosion equation formalizes the conceptual model as

$$\frac{\partial \eta}{\partial t} = -\frac{1}{C_b}\left(\frac{\partial (Q_{s_x} + Q_{b_x})}{\partial x} + \frac{\partial (Q_{s_y} + Q_{b_y})}{\partial y} + \frac{\partial V_s}{\partial t}\right) \quad (1)$$

where η is bed elevation, t is time, C_b is the volume concentration of sediment in the bed, Q_s and Q_b are the volume rates of suspended load and bedload sediment transport, x is the cross-shore direction, y is the alongshore direction, V_s is the volume of sediment per unit area of bed in the water column. The LHS of Eq. (1) is the rate of change in bed level. The negative sign appears before RHS of the equation because the bed erodes when $\frac{\partial (Q_{s_x}+Q_{b_x})}{\partial x}$, the gradient in cross-shore sediment transport is negative (more sediment coming in than leaving), $\frac{\partial (Q_{s_y}+Q_{b_y})}{\partial y}$ is negative, or $\frac{\partial V_s}{\partial t}$ is negative (sediment falling to the bed).

The erosion equation is fundamental to formulating a model of tsunami sedimentation. Erosion or deposition during a tsunami can be calculated by solving the RHS of Eq. (1). Conversely, sediment transport during the tsunami can be calculated by measuring bed elevation change resulting from the tsunami and solving for gradients in transport and change in sediment volume in the water column.

To simplify the model, we assume that the sediment transport during a tsunami that is reflected in tsunami deposits can be modeled as a steady process (Fig. 2). This and the other simplifying assumptions below are discussed in Section 6.1. Although the flow may be turbulent, we assume that the mean flow is steady because the temporal gradients in mean flow speed (i.e., when averaged over the turbulent fluctuations) during much of the tsunami inundation landward of the shoreline are small. This assumption is violated when a tsunami first transports sediment as it inundates land and at the time when the tsunami reaches its maximum inland extent when flow decelerates. However, near the peak of the tsunami, because tsunami periods are long, the temporal change in flow speed is small and the flow can be approximated as steady. We assume that the tsunami deposits contain sediments that charged the water column to its full capacity during the steady portion of the flow.

We also assume that for some tsunamis, the sediment transport can be modeled as quasi-spatially uniform (small horizontal gradients in transport). This assumption is violated near the limit of inundation where

sediment transport goes to zero and near the shoreline where the tsunami is spatially accelerating. However, away from the limit of inundation in locations where topography is slowly varying, horizontal gradients in sediment transport can be small and not significantly contribute to formation of tsunami deposits.

Finally, we can assume that for many tsunamis the contribution of bedload to the formation of the deposits is small relative to the contribution of suspended load. This assumption is violated where the ratio of sediment settling velocity over the product of von Karman's constant and the shear velocity is large (greater than about 2) and there is little or no suspended load transport. However, where sediment transport is large, we assume that the tsunami deposit reflects primarily suspended load transport. Based on estimates of tsunami flow speed from this work and others (Matsutomi in Kawata, 1999) and sediment grain size, estimates of bedload transport rates are less than 10% of the total transport.

Where the assumptions of steady, uniform flow and suspended load dominating formation of deposits are valid, Eq. (1), in its discrete form, reduces to

$$\Delta\eta = -\frac{1}{C_b}\int_{bed}^{surface} C_s(z)\mathrm{d}z \tag{2}$$

where C_s is the suspended sediment volume concentration and z is elevation above the bed. The LHS of Eq. (2) is the thickness of the tsunami deposit and the RHS is the bed porosity correction times the volume of suspended sediment in the water column during the steady portion of the tsunami. Where the above assumptions are valid, local tsunami flow speed can be calculated using a simple sediment transport model to determine flow speeds necessary to suspend the volume and size of sediment to create observed tsunami deposit thickness and grain size distribution. Conditions under which these assumptions may be valid will be examined in detail in the Discussion section of this paper.

2.3. Model for estimating tsunami flow speed from a tsunami deposit

Tsunami flow speed is calculated by matching the sediment suspended by the tsunami with the thickness and grain size distribution of the tsunami deposit. In turbulent steady uniform flow, downward settling of sediment is balanced by upward mixing resulting in a steady concentration profile described by:

$$C_i(z) = C_{r_i} e^{w_{s_i}\int_{z_{o_{total}}}^{z}\frac{1}{K(z)}\mathrm{d}z} \tag{3}$$

where $C_i(z)$ is the sediment concentration of size class i at elevation z above the bed, C_{r_i} is the reference concentration for size class i, w_{s_i} is the sediment settling velocity, z_o is the bottom roughness parameter, and K is the eddy viscosity (a function of U^*, the shear velocity and distance above the bed).

Reference concentration is calculated following Madsen et al. (1993) as

$$C_{r_i} = \frac{\gamma_0 C_b f_i S}{1+\gamma_0 S} \tag{4}$$

in which γ_0 is the resuspension coefficient, C_b is bed concentration, f_i is the fraction of bed sediment in size class i, and S is normalized excess shear stress given by

$$S = \frac{\tau_b - \tau_{cr_i}}{\tau_{cr_i}} \qquad \tau_b > \tau_{cr_i} \tag{5a}$$

$$S = 0 \qquad \tau_b \le \tau_{cr_i} \tag{5b}$$

where τ_b, the bed shear stress, is

$$\tau_b = \rho_w U_*^2 \tag{6}$$

with ρ_w the density of water and U^* the shear velocity, and the critical shear stress for the initiation of motion is

$$\tau_{cr} = \rho_w U_{*_{cr_i}}^2 \tag{7}$$

where $U_{*_{cr_i}}$ is the critical shear velocity for initiation of motion for size class i.

To calculate reference concentration, we must choose a method for calculation of $U_{*_{cr_i}}$ and values for γ_0 and C_b. We calculate $U_{*_{cr_i}}$ following Madsen et al. (1993). We use the Hill et al. (1988) value of 1.4×10^{-4} for γ_0 and 0.65 for C_b (Smith and McLean, 1977).

To solve Eq. (3), sediment settling velocity, bottom roughness, and eddy viscosity must be specified. Settling velocity is calculated from sediment grain size following Dietrich (1982), using a Corey Shape Factor (Corey, 1949) of 0.7 and a Powers roundness value (Powers, 1953) of 3.5.

The approach of Wieberg and Rubin (1989) is used to calculate bed roughness. Bed roughness, $z_{o_{total}}$, is the combination of a Nikuradse bed roughness (Nikuradse, 1933), z_{o_N}, and a roughness created by saltating sediment, z_{o_S}.

$$z_{o_{total}} = z_{o_N} + z_{o_S} \tag{8}$$

The Nikuradse bed roughness is

$$z_{o_N} = \frac{\overline{d}}{30} \tag{9}$$

where $\overline{d}$ is the mean grain diameter. The roughness from saltating sediment is

$$z_{o_S} = \alpha_{WS}\delta_b \tag{10}$$

where α_{WS} is a constant equal to 0.056 and δ_b is the average saltation height, which is a function of boundary and critical shear stresses, using the formula from Wieberg and Rubin (1989).

Eddy viscosity, K, is given by Gelfenbaum and Smith (1986) as

$$K(z) = kU_* z e^{\frac{-z}{h} - 3.2\left(\frac{z}{h}\right)^2 + \frac{2}{3}3.2\left(\frac{z}{h}\right)^3} \tag{11}$$

where k is von Karman's constant, 0.41, and h is flow depth. This formulation was developed as a best fit to laboratory data collected under steady uniform flow conditions.

The model iteratively adjusts sediment source distribution and shear velocity (a parameterization of turbulent mixing intensity) to match the observed bulk grain size distribution and thickness of the tsunami deposit. For the first calculations, a guess of the shear velocity that created the deposit and the tsunami deposit bulk grain size distribution is used in Eqs. (3)–(10). For each size class, the reference concentration, suspended sediment profile, and total suspended load are calculated. The thickness and grain size distribution of the deposit created from this sediment settling from suspension are compared to the observed deposit. If the modeled deposit does not match the observed deposit with the desired accuracy, the shear velocity and bed grain size distribution are adjusted to create the observed deposit. Shear velocity is increased (decreased) if the modeled deposit is too thin (thick). Likewise, the fraction in each bed grain size class is increased (decreased) if the fraction in suspension is smaller (greater) than that in the observed deposit. Adjustment of shear stress and grain size classes is alternated. Total bottom roughness is also adjusted during each iteration. The model is run until both the sediments in suspension for each size class match the fraction observed in the deposit and the deposit thickness matches the observed thickness to within 1%. If the initial guess for shear velocity does not result in model convergence, a new guess is made and the model is rerun. For runs on modern tsunami deposits, the model is not sensitive to the initial guess in shear velocity; however, if the deposit was not formed by sediment settling from suspension, the model does not converge because the size distribution in the deposit is not reproducible by this model.

After determining the shear velocity needed to produce the deposit, the flow speed profile, $U(z)$, is calculated by

$$U(z) = \int_{z_{o\,\mathrm{total}}}^{z} \frac{U_*^2}{K(z)}\mathrm{d}z \tag{12}$$

using numerical integration. The depth averaged flow speed, calculated as the integral of Eq. (12) divided by the flow depth, is reported in the remainder of the paper.

3. Sensitivity analysis

The above tsunami sediment transport model, referred to as TsuSedMod, could use different formulations and values of model parameters. We explore TsuSedMod sensitivity to choices of eddy viscosity profile, bottom roughness formulation, and resuspension coefficient. TsuSedMod also requires three inputs: grain size distribution, deposit thickness, and tsunami flow depth. TsuSedMod sensitivity to variations in flow depth, a poorly constrained input, especially for paleotsunamis, is examined. The effect of variation in grain size distribution and deposit thickness, both measured from the tsunami deposit at the location where the estimate of flow speed is made, will be explored in detail in the Tsunami flow speed section.

Sensitivity of TsuSedMod to changes in the above model parameters and choices is calculated on variations about a base case chosen from field data. Tsunami deposit thickness reported for modern tsunamis (Shi et al., 1995; Sato et al., 1995; Nishimura and Miyaji, 1995; Bourgeois et al., 1999; Gelfenbaum and Jaffe, 2003; Jaffe et al., 2003) ranges from 0.5 cm near the limit of inundation to about 50 cm. A typical value for deposit thickness is 10 cm, which is the value chosen for the base case. Grain size of modern tsunami deposits is also variable in the shore-normal direction, fining towards the limit of inundation (Shi et al., 1995; Nishimura and Miyaji, 1995; Gelfenbaum and Jaffe, 2003; Moore et al., 2006). A fine sand with a mean grain diameter of 0.15 mm (2.74 phi) is used for the base case presented here. A tsunami flow depth of 5 m is also used for the base case.

3.1. Model parameters

3.1.1. Eddy viscosity profile

The vertical variation of turbulent stress within a tsunami inundating over land is not well known.

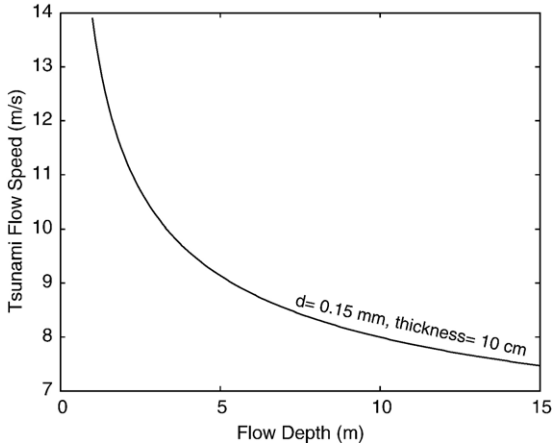

Fig. 3. Calculated tsunami flow speed as a function of flow depth for a 10-cm-thick deposit composed of 0.15 mm sand with a particle density of 2.65 g/cm^3.

Fortunately, the choice of the eddy viscosity profile shape, which parameterizes the vertical variation in turbulent stress, does not strongly influence the estimate of average tsunami flow speed calculated by TsuSedMod. Sensitivity of tsunami flow speed to eddy viscosity profiles is tested for three eddy viscosity profile shapes, a linear eddy viscosity profile, $K(z)=kU*z$; a parabolic viscosity profile, $K(z) = kU*z\left(1-\frac{z}{h}\right)$; and a profile that is a best fit to steady, uniform flow laboratory data, which is given by Eq. (11) (Gelfenbaum and Smith, 1986). For the base case of 0.15 mm grain size, flow depth of 5 m, and deposit thickness of 10 cm, calculated tsunami speeds are 7.8 m/s (linear profile), 8.8 m/s (parabolic), and 9.1 m/s (Gelfenbaum and Smith profile). Turbulent mixing of sediment into the water column is less using the Gelfenbaum and Smith eddy viscosity profile — a greater average flow speed than the other two profile choices (14% greater than for linear profile, 3% greater than parabolic profile) is needed to suspend the amount of sediment deposited.

3.1.2. Bed roughness

The estimate of flow speed from tsunami deposit characteristics is relatively insensitive to bed roughness. For the base case tsunami deposit, bed roughness calculated from combined grain and sediment transport roughness (Wieberg and Rubin, 1989) is 2.17×10^{-5}. Increasing (decreasing) bed roughness by an order of magnitude decreases (increases) average flow speed by 25%.

3.1.3. Resuspension coefficient

The estimate of tsunami flow speed is sensitive to the choice of resuspension coefficient. Resuspension coefficient influences the reference concentration (Eq. (4)), which scales the amount of sediment in suspension in the water column. The resuspension coefficient remains one of the poorest known parameters in sediment transport. Values reported in the literature vary from 10^{-5} to 10^{-3} for continental shelves and estuaries (Drake and Cacchione, 1989; Vincent et al., 1991). An increase in the resuspension coefficient from 10^{-4} to 10^{-3} decreases the tsunami flow speed needed to create the base case tsunami deposit by 44%. A decrease in the resuspension coefficient from 10^{-4} to 10^{-5} increases the tsunami flow speed needed to create the standard tsunami deposit by 120%. The effect of changing resuspension coefficient is greater for smaller values because suspended sediment concentration decays exponentially with elevation above the bed. At lower values of γ_0, the decrease in reference concentration from a small change in γ_0 must be compensated by greatly increased mixing to suspend the same quantity of sediment in the water column.

3.2. Input parameters

3.2.1. Flow depth

TsuSedMod is not sensitive to flow depth for the same deposition until the flow is relatively shallow (Fig. 3). This insensitivity is because there is an exponential decay in suspended sediment concentration with elevation above the bed (Eq. (3)). Most of the sediment in suspension is near the bottom; decreasing (increasing) depth when the flow is deep removes (adds) water with relatively little suspended sediment. A 1-m change in a flow depth of 10 m results in 4% change in mean flow speed calculated from the same deposit. Decrease in depth from 15 to 5 m increases mean flow speed by only 22%. A depth decrease from 2 to 1 m, however, has a larger effect, increasing flow speed by 23%. Tsunami flow depth is often either unknown (paleotsunami deposits) or poorly constrained (most modern tsunami deposits). Flow depth can be specified using a variety of means, including geologic reconstructions (elevations of overtopped coastal dunes), or relations between flow depth and tsunami speed (e.g. Froude number). The use of Froude number to constrain the flow depth input to TsuSedMod is addressed in the Discussion section.

4. Tsunami flow speed

To calculate tsunami flow speed, TsuSedMod iteratively adjusts sediment source distribution and shear velocity (used to calculate sediment pick-up, turbulent mixing intensity, and bed roughness) to match the observed bulk grain size distribution and thickness

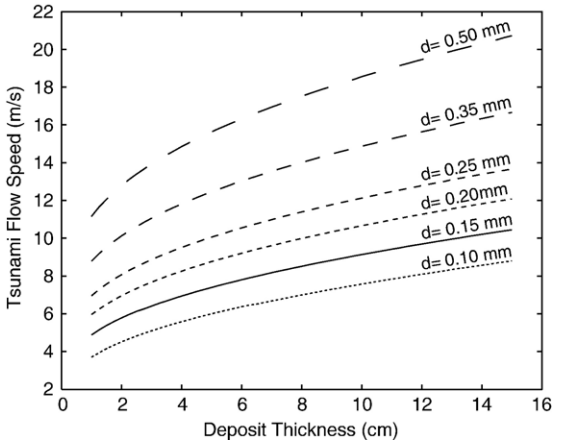

Fig. 4. Calculated tsunami flow speed as a function of deposit thickness for deposits with grain sizes ranging from 0.10 to 0.50 mm and a particle density of 2.65 g/cm^3.

of the tsunami deposit. After determining the shear velocity needed to produce the deposit, flow velocity is calculated using Eq. (12). We present results from the idealized case of a tsunami deposit composed of a single grain size and from a test case where the model is applied to field and laboratory measurements of tsunami deposits formed during the 1998 Papua New Guinea tsunami as reported in Gelfenbaum and Jaffe (2003).

4.1. Idealized case: single grain size tsunami deposits

4.1.1. Deposit thickness

TsuSedMod predicts faster tsunami flow speeds which responsible for thicker tsunami deposits. Tsunami flow speeds for deposits from 1 to 15 cm thick, with grain sizes from 0.10 to 0.5 mm, and a particle density of 2.65 g/cm^3 are shown in Fig. 4. Tsunami flow speed is not a strong function of deposit thickness. For example, for a deposit with 0.15 mm sand that was formed in a 5 m deep flow, a 1 cm (10%) change in thickness of a 10 cm deposit results in a 3% change in tsunami flow speed. Thinner deposits (2 cm) changed by 1 cm result in only an 18% decrease (thinner) or 11% increase (thicker) in tsunami flow speed.

4.1.2. Grain size

Grain size of a tsunami deposit has a strong influence on calculated flow (Fig. 5). For example, for a 10-cm-thick deposit formed in 5 m flow depth, a 10% change in grain size of 0.15 mm results in a 5% change in mean flow speed. Because the natural variation in grain size of source sediment can be large, grain size of the deposit can be the most significant factor in determining tsunami flow speed. A deposit of a given thickness, with a particle density of 2.65 g/cm^3, composed of coarse sand (d=0.5 mm) is created by a flow speed 2 to 3 times greater than the one composed of very fine sand (d=0.0625 mm).

4.2. Test case: 1998 Papua New Guinea tsunami deposits

On the evening of July 17, 1998 a magnitude 7.0 earthquake was followed by a series of tsunami waves that devastated villages on the north coast of Papua New Guinea (PNG) (Kawata et al., 1999). The confirmed death toll was over 2200, and coastal villages located on barrier spits around Sissano Lagoon were totally destroyed. The tsunami consisted of three large waves, the first making land fall approximately 20 min after coastal residents felt the earthquake (Davies, 1999). The second came within 5 min of the first wave and the third wave came within 5 min of the second wave. According to eyewitnesses, the second and third waves flowed over the low-lying coast before the first wave completely receded, causing an additive effect in water level. Waves ripped large trees out of the ground by the roots and moved both traditional wooden and modern brick and mortar structures off of their pilings or foundations tens to hundreds of meters away into the lagoon (Fig. 6).

Tsunami deposit and flow depth data collected in September 1998 from the Arop transect located about 500 m east of Sissano Lagoon (Gelfenbaum and Jaffe, 2003) are used to evaluate TsuSedMod performance. The Arop transect was chosen as the test case because of its simple topography (Fig. 7A) and tsunami deposit geometry (Fig. 7B), predominance of normally graded single layer deposits (e.g. Fig. 1), presence of a wide

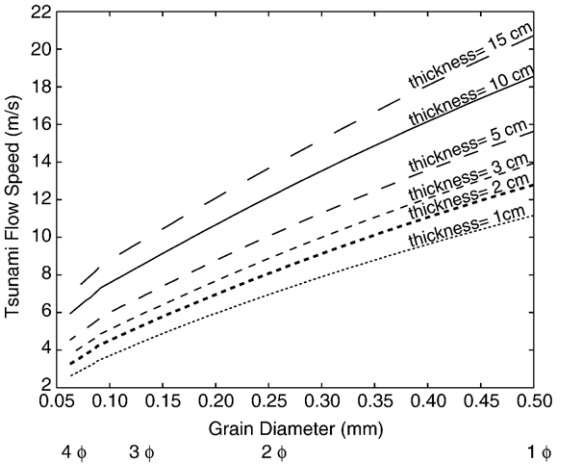

Fig. 5. Calculated tsunami flow speed versus grain size for deposits 1–15 cm thick with a particle density of 2.65 g/cm^3.

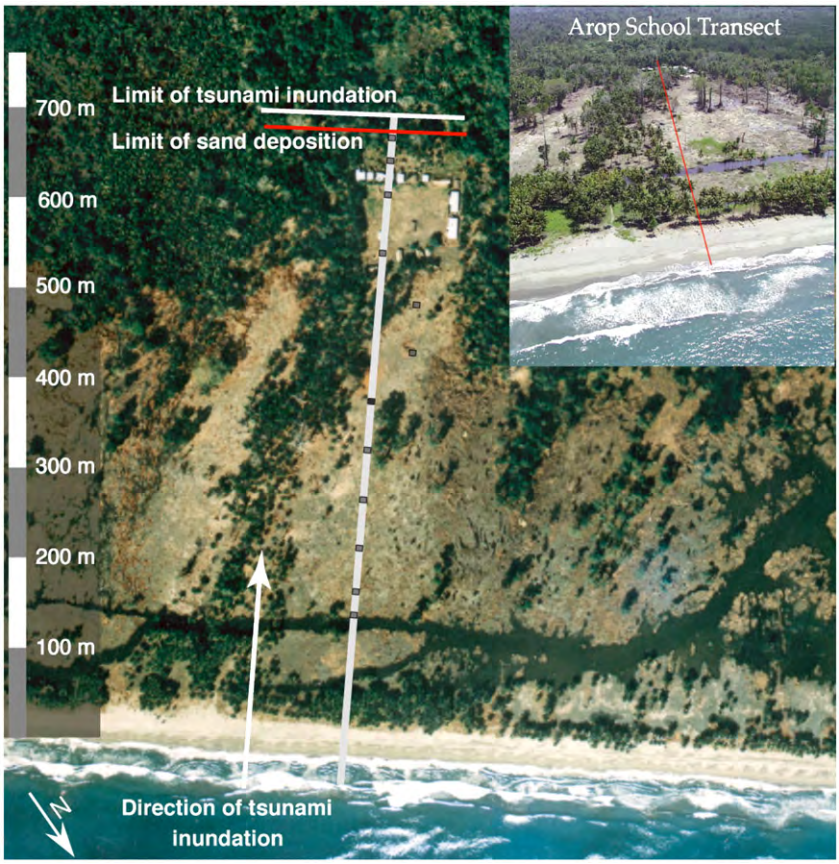

Fig. 6. Aerial photograph and oblique aerial photograph (inset) of Arop, Papua New Guinea transect. Trenches where TsuSedMod was run to calculate tsunami flow speed from tsunami deposits are shown as squares. Figure modified from Gelfenbaum and Jaffe (2003).

zone from about 150 to 500 m inland with fairly constant grain size texture (Fig. 7C), and the high-quality flow depth indicators (Fig. 7D). There are also two independent estimates of tsunami flow speed from this location (Titov et al., 2001; Matsutomi in Kawata, 1999).

Field measurements of tsunami deposit thickness (Fig. 7B) and laboratory measurements of deposit bulk grain size distribution (Fig. 8) from field samples are used as input to TsuSedMod. Particle settling velocity was measured in 2-m-long settling tubes for sand sized sediment, and calculated following Dietrich (1982) using a particle density of 2.65 g/cm^3 for finer sediment that was run through a laser-diffraction particle analyzer. Because of the strong dependence of tsunami flow speed on grain size, measurements were made at 1/4-phi intervals.

Flow depths used in model runs were based on field measurements (Fig. 7D) (Gelfenbaum and Jaffe, 2003; Kawata, 1999). Field evidence (broken branches, water marks, debris caught in branches, sediment deposited on floors of buildings) yields minimum estimates of the peak flow depth. Underestimating flow depth results in higher calculated tsunami speed (Fig. 3).

Flow speeds calculated by TsuSedMod are shown in Fig. 7E. Because flow depth was not well constrained by field measurements, a range of flow speeds based on a 20% uncertainty in flow depth at each location are shown. Calculated flow speed decreases from approximately 14 m/s at 200 m inland to approximately 10 m/s at 600 m inland. The decrease is not monotonic, with speeds lower than a linear trend at 300–350 m inland and higher than the trend at approximately 500 m inland. It is not known whether this variation reflects actual changes in tsunami flow speed, poor model performance because of violation of model assumptions (e.g.; uniform flow), or a combination of the two causes. If horizontal flow decelerations were large enough to result in significant deposition (Eq. (1)), using the grain size and thickness of the entire tsunami deposit for modeling would overestimate flow speeds. The flow speeds landward of 600 m inland are shown in gray because they are likely overestimates because we expect

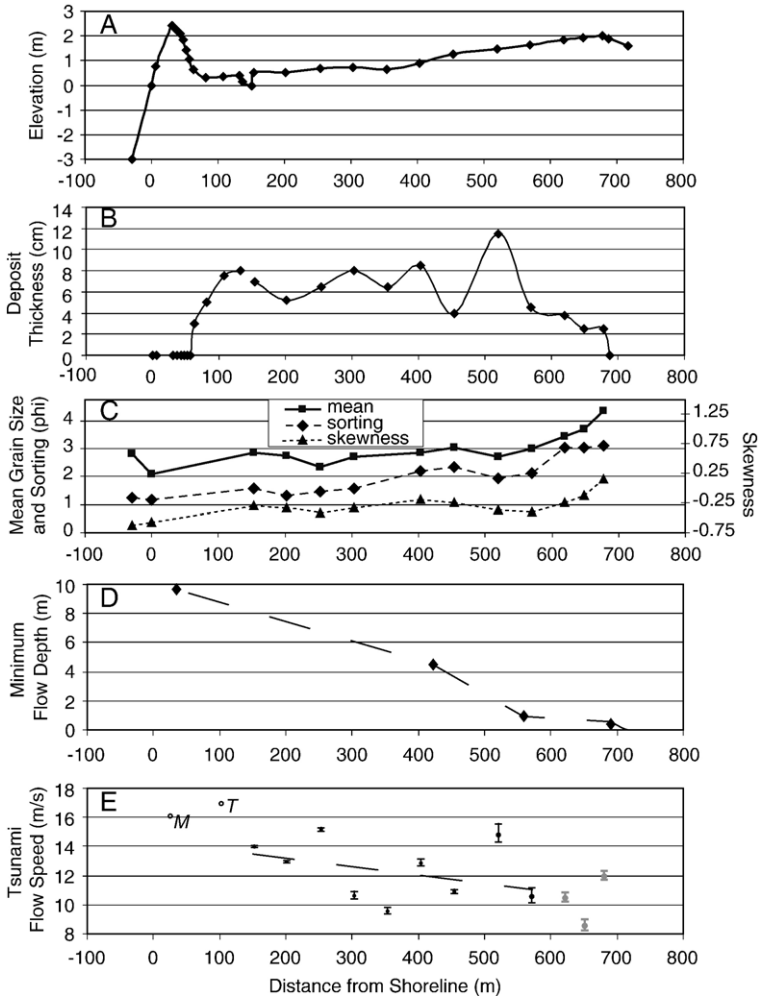

Fig. 7. TsuSedMod inputs and calculated tsunami flow speed at Arop, Papua New Guinea transect. Elevations (relative to mean sea level) in panel A, deposit thicknesses in panel B, and grain size statistics in panel C are from Gelfenbaum and Jaffe (2003). The range of calculated tsunami flow speeds shown in panel E is for a 20% uncertainty in flow depths shown in panel D. The dashed line, which is a least squares fit to the calculated flow speeds, shows a landward decrease in flow speed. Calculated flow speeds landward of 600 m inland are shown in gray because they are likely overestimates because we expect the tsunami to be strongly decelerating, violating the uniform flow assumption, as it nears the limit of inundation. Tsunami flow speed estimates by Titov et al. (2001) and Matsutomi (in Kawata, 1999) are indicated by open circles labeled with a "T" and "M", respectively, in panel E. These estimates are within 20% of the calculated flow speed 200 m inland, suggesting that the assumptions used in developing TsuSedMod are valid and the model is able to estimate tsunami flow speed from sedimentary deposits for this tsunami.

the tsunami to be strongly decelerating, violating the uniform flow assumption of the model, as it nears the limit of inundation. The flow speed approximately 500 m inland, which is in the region where field measurements show flow depth decreasing over a short distance, could also be too high if a significant part of the deposit was formed by convergence in sediment transport.

Two other independent estimates of tsunami flow speed are compared to the estimates from the tsunami deposits (Fig. 7E). Titov et al. (2001) used the MOST 1-D inundation model (Titov and Synolakis, 1998) to calculate land tsunami flow speed from offshore wave characteristics propagated over measured bathymetry and topography. Their estimate for the peak flow speed at 100 m inland is 17 m/s. Matsutomi (in Kawata, 1999) calculated tsunami flow speed using Bernoulli's principle and water level data on buildings left standing after the tsunami. His estimate of peak flow speed on the spit at approximately 50 m inland is 16 m/s. The similarity of these two estimates, within 10 to 20%, to flow speeds calculated at approximately 200 m inland using TsuSedMod indicates

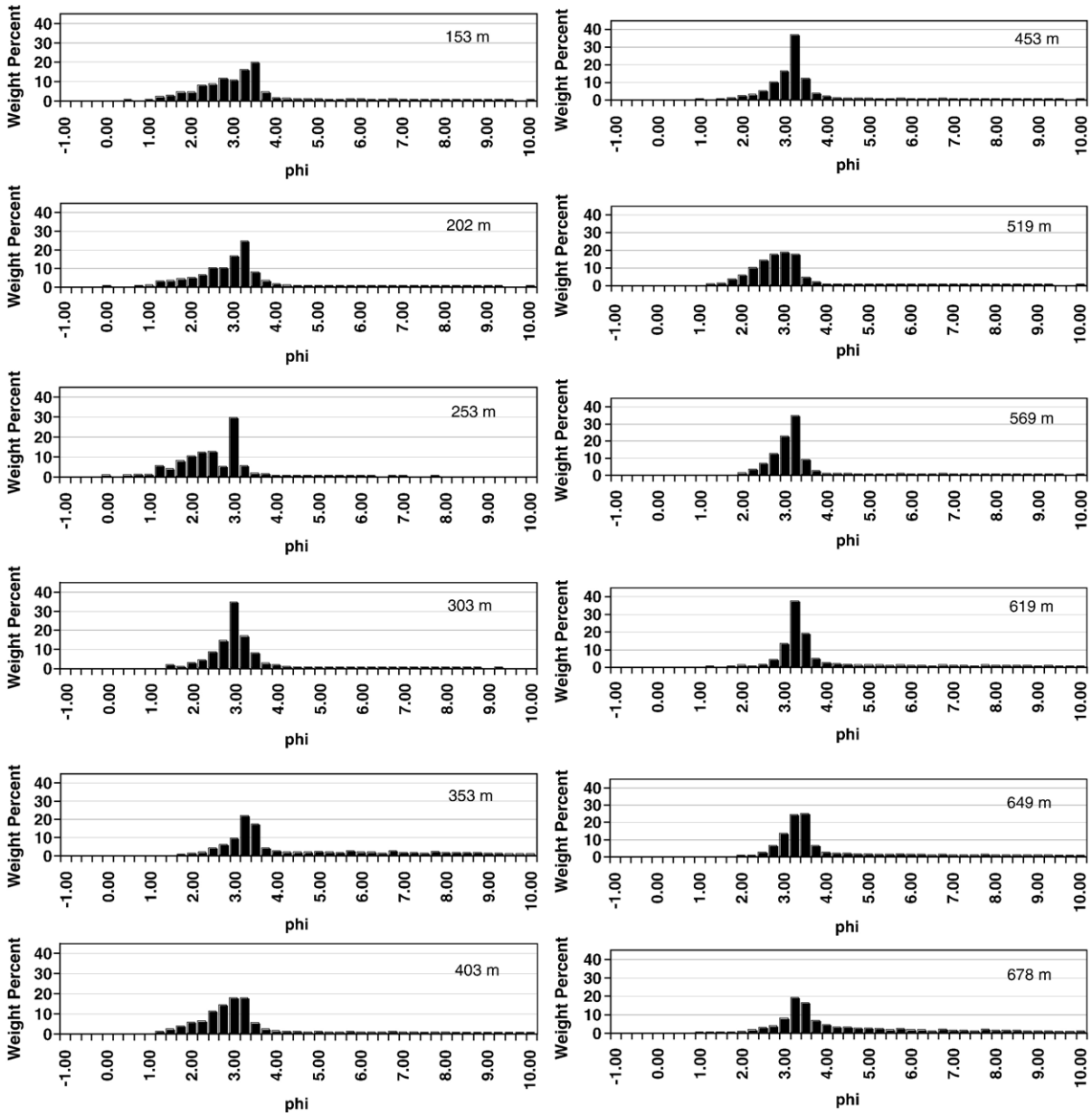

Fig. 8. Tsunami deposit bulk grain size at Arop, Papua New Guinea transect used as input to TsuSedMod. Numbers on graphs (e.g.; 153 m) are the locations of the tsunami deposit in distance inland from the shoreline in meters.

that model assumptions are likely valid and the model is able to estimate tsunami flow speed from characteristics of the tsunami deposits.

5. Tsunami deposit grading

To check a key model assumption, that tsunami deposits are formed by settling from suspension, we compared the vertical variation in grain size of the deposit 403 m inland at Arop to a synthetic deposit constructed by allowing sediment suspended by the model to settle to the bed. This is not an entirely independent test — the starting point for these calculations of bed grading is sediment in suspension, which is forced by TsuSedMod to match the total volume and bulk grain size of the observed deposit. However, it is an independent test in that there are no constraints on how TsuSedMod distributes the sediment in the water column and the observed grading is additional

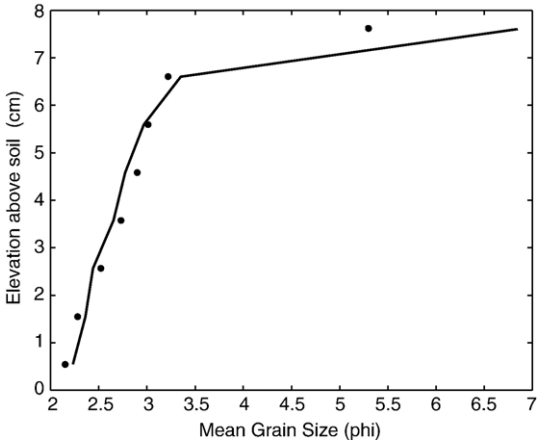

Fig. 9. Comparison of predicted (line) and observed (circle, sediment samples collected at 1-cm intervals in the field and analyzed for grain size in the laboratory) grading at Arop at a location 403 m inland from the shoreline. Predicted deposit constructed by allowing sediment suspended by the model to settle to the bed. The decrease in grain size in the deposit matches that predicted by settling of sediment distributed in the water column in concentrations creating equilibrium profiles for all the size classes (Eqs. (3) and (4)) at the shear velocity necessary to reproduce the bulk grain size and thickness of the tsunami deposit observed at this location. The fine sediment at the top of the deposit results from its low settling velocity and the tendency for it to be mixed higher up in the water column than coarser sediment. The match between predicted and observed grading supports the assumption that the deposit formed from sediment falling out of suspension.

data not inputted into the model. If the deposit formed by some process other than settling from suspension, we would not expect the vertical variation in grain size predicted by settling to match the observed grading. In addition, we do not expect that deposition by bedload would create a normally graded deposit with the same decrease in grain size higher in the deposit as observed unless the sediment source was fining with time in a complex manner that mimicked the observed grading. Fig. 9 shows a good match between predicted and measured vertical grading in the deposit. The decrease in grain size upwards in the deposit matches that predicted by settling of suspended sediment that was distributed in the water column in equilibrium profiles for all the size classes (Eqs. (3) and (4)) using the shear velocity necessary to reproduce the bulk grain size and thickness of the tsunami deposit observed at 403 m inland at Arop. The much finer sediment at the top of the tsunami deposit in both the observed and calculated deposits results from the slow settling velocities of the fine sediment and the tendency for fine sediments to be mixed higher up in the water column. The trends and magnitudes in vertical variation of predicted and observed sorting (average difference of 0.1 phi) and skewness (average difference of 0.2 phi) are also similar. Vertical variation in grain size in the deposit at 403 m inland is consistent with formation by settling from suspension.

6. Discussion

6.1. Model limitations

A key assumption of the model, that deposits are formed by sediment falling out of suspension, is supported by field observations of normal grading (Shi et al., 1995; Sato et al., 1995; Nishimura and Miyaji, 1995; Bourgeois et al., 1999; Gelfenbaum and Jaffe, 2003; Jaffe et al., 2003) and the ability of TsuSedMod to reproduce the observed vertical variation in grain size at 403 m inland at Arop, Papua New Guinea (Section 5). However, inverse grading and complex grading (Shi et al., 1995; Jaffe et al., 2003), indications that a deposit was not solely formed by settling from suspension, are also observed in modern tsunami deposits. This model is not applicable under conditions where a deposit is not formed from suspension and should not be applied to such locations.

The conditions under which sediment transport is spatially uniform (does not form a deposit from convergences in sediment transport) are violated where the tsunami speed decreases rapidly as it moves inland. TsuSedMod, which does not include formation of tsunami deposits from horizontal convergences in sediment transport, is not strictly applicable at these locations. However, if the deposits formed from convergences in sediment transport were thin relative to the entire deposit thickness, the overestimate in tsunami flow speed would not be significant because the model is relatively insensitive to deposit thickness (Fig. 4). An exception to this is if the portion of the deposit formed by convergences contains larger diameter grains than the remainder of the deposit. TsuSedMod is sensitive to grain size and assuming these large grains were deposited from suspension could result in a significant overestimate of tsunami flow speed.

To explore the potential contribution of convergences in sediment transport to formation of deposits, we calculated suspended load and bedload fluxes at the location 403 m inland at Arop, Papua New Guinea. The shear velocity calculated by TsuSedMod is 0.41 m/s — an extremely large value compared to shear velocities in other flows observed in nature (Drake and Cacchione, 1989; Vincent et al., 1991). Calculated suspended load fluxes are 12 to 18 times greater than bedload flux calculated using the bedload model of Meyer-Peter and Muller (1948) and a modified version for higher bed

stresses (still much lower than the bed stress in a large tsunami) given in Nilsen (1992). Because suspended load flux is an order of magnitude greater than bedload flux, it has the potential to contribute more to deposit formation; although, convergences would not be exactly proportional to flux. The much greater transport of sediment in suspension also underscores the need for any tsunami sediment transport model to represent suspended sediment transport as accurately as possible. If the goal is to model small tsunamis where shear stresses are small (bedload component comparable or larger than suspended load), TsuSedMod may not be the appropriate model to use.

The assumption of steady flow is violated at the leading edge of the tsunami and when the tsunami uprush stops. The temporal acceleration as the leading edge passes will result in erosion, if the substrate is erodible and the stress is greater than the critical stress for erosion. This erosion does not affect the calculated tsunami flow speed. The long period of tsunami waves results in slowly varying flow speed near the peak of the tsunami. This peak speed is what TsuSedMod calculates. If the decay in speed is slow and the sediment is continuously depositing rather than all depositing from the flow stopping abruptly, as is assumed here (Fig. 2), the details of the vertical grain size in the deposits will be altered, but unless there are spatial flow convergences or a change in grain size in sediment source that accompany the slow decay in speed, we expect the model to still be applicable. This is because the model uses the total thickness and bulk grain size of the tsunami deposit.

6.2. Deposit thickness

Deposit thickness alone is not a good indicator of tsunami flow speed (Fig. 4) because small changes in flow speed result in large changes in the concentration of sediment in the water column. For a given grain size, the concentration of sediment in suspension near the bed goes as the square of the shear velocity (Eqs. (4) (5a) (6)). The sediment concentration higher in the water column varies with eddy viscosity (Eq. (3)), which parameterizes mixing and is a function of the shear velocity (Eq. (11)). The combination of the sensitivity of concentration near the bed and in the water column to shear velocity results in large changes in deposit thickness for a small change in shear velocity. For the inverse problem, the relative insensitivity of tsunami flow speed, the parameter of interest, is fortuitous because spatial variability in tsunami deposit thickness on the order of a few centimeters can occur over horizontal distances on the order of a few meters (Gelfenbaum and Jaffe, 2003; field observations by the authors in Sumatra and Sri Lanka after the 26 December 2004 Indian Ocean Tsunami).

6.3. Deposit grain size

A question not commonly asked, but which should be, to gauge how large (fast) the tsunami was that created a deposit is “what is the grain size of the deposit?” Tsunami flow speed calculated from the deposit is very sensitive to grain size (Fig. 5) and, for deposits composed of many grain sizes, to the bulk grain size distribution. Grain size is important because the amount of sediment in suspension is a function of the critical shear velocity for the initiation of motion (Eqs. (3)–(5a), (7)) and the settling velocity (Eq. (3)), both of which vary with grain size. A small change in grain size results in a large change in the shear velocity (tsunami speed) necessary to create a deposit of the same thickness.

It is important to point out that Figs. 4 and 5 are not intended to be used for estimating tsunami flow speed (tsunami height) using the mean grain size alone. Naturally occurring tsunami deposits are not composed of a single grain size. The coarser grains in the distribution influence calculated tsunami flow speed more than the fine grain sizes — using the mean size, for instance, would result in a significant underestimate of tsunami flow speed even for well-sorted sediments. For example, the flow speed calculated from a deposit with a mean grain size of 0.137 mm (2.87 phi), which is the mean grain size of the deposit approximately 400 m inland at Arop, is 5.5 m/s; flow speed calculated using the complete distribution of grain sizes (Fig. 8) is 12.7 m/s. Therefore, it is very important to use the complete grain size distribution of the deposit, including the coarse grain tail, with this model.

6.4. Model improvements

TsuSedMod can be improved to be more generally applicable for reconstructing tsunami characteristics from the sedimentary deposits left behind. Improvements to the model can be made for determining tsunami characteristics using deposits from a single location, the approach now used, and using deposits from multiple locations.

Possible additions to a model using deposits at a single location include the ability to calculate tsunami flow depth, and the ability to calculate flow speeds from deposits formed during unsteady and non-uniform flow. The details of the grading of tsunami deposits could

possibly constrain the tsunami flow depth. The grading in the upper portion of tsunami deposits will be stronger for greater flow depths because sediment grains will segregate more by settling velocity as they settle from higher up in the water column. It is not known whether our incomplete knowledge of the vertical distribution of the turbulent mixing intensity would severely limit the utility of this approach. Another approach to constraining tsunami flow depth is to use the Froude number, the ratio of the tsunami flow speed to the wave speed, $\frac{U}{\sqrt{gh}}$. The flow speed calculated from TsuSedMod and knowing the Froude number define the flow depth. In the laboratory, tsunami Froude numbers range from 1 to 2 (Yeh et al., 1989). Tsunami Froude numbers, estimated from field measurements and theory, for five recent tsunamis range from 0.7 to 2.0 (Matsutomi in Kawata, 1999). As more becomes known about variation of tsunami Froude numbers in nature, tsunami deposits can be used to calculate tsunami flow depth as well as tsunami flow speed.

Coupling TsuSedMod with an inundation model will allow the inclusion of flow unsteadiness and non-uniformity in formation of tsunami deposits. The contribution of sediment transport convergences and unsteady sediment transport to formation of a tsunami deposit at a single location can be modeled. The inverse problem, estimating tsunami flow speed from a tsunami deposit, can also be done more completely.

Adding the ability to use grain size and thickness of deposits from multiple locations will generalize the model. A next generation model that evaluates sediment transport convergences and flow unsteadiness from the inland change in grain size of deposits will allow calculation of tsunami flow speed at locations where TsuSedMod is not appropriate. The cross-shore distribution of the volume for each grain size of the sediment deposited can also be used to constrain sediment fluxes, which has the potential to give information about the period of the tsunami that formed the deposit. As with using deposits from a single location, coupling a multiple location sediment transport model with an inundation model is a promising area of research for expanding the ability to interpret tsunami characteristics from the deposit it leaves behind.

7. Summary

A simple model for tsunami sedimentation is developed and applied to calculate tsunami flow speed from the thickness and grain size of a tsunami deposit. Under certain conditions, tsunami sediment transport can be modeled as a steady, spatially uniform process. Tsunami deposits form as sediment suspended during the peak of the tsunami rains out of the water column when the on-land tsunami flow speeds are zero everywhere as the tsunami reaches its maximum inundation. Tsunami flow speed is calculated from the shear velocity that is necessary to suspend the quantity and grain size distribution of the sediment observed in the deposits.

For an idealized deposit composed of a single grain size, grain size of the deposit is a better predictor of tsunami flow speed than deposit thickness. For deposits 10 cm thick composed of 0.15 mm sand, a 10% change in thickness results in a 3% change in tsunami flow speed. For deposits composed of 0.15 mm sand that are 10 cm thick, a 10% change in grain size results in a 5% change in tsunami flow speed.

Flow speeds for the 1998 Papua New Guinea tsunami calculated using the simple model presented here compare favorably (within 10–20%) with estimates from application of Bernoulli's principle to water levels on buildings (Matsutomi in Kawata, 1999) and an inundation model (Titov et al., 2001). These favorable comparisons suggest that the assumptions made to develop this model are applicable in, at least, these conditions.

The simple model is also able to reproduce observed grading in a tsunami deposit created by the 1998 Papua New Guinea tsunami at a location 403 m inland from the shoreline. The trends and magnitudes in vertical variation of predicted and observed sorting (average difference of 0.1 phi) and skewness (average difference of 0.2 phi) are also reproduced by the model.

Modeling formation of tsunami deposits has the potential to greatly improve understanding of both modern and paleotsunamis. Additional research is needed to further develop the simple model presented in this paper to increase the information on tsunami characteristics that can be determined from tsunami deposits.

Acknowledgements

The numerical model is based on MATLAB code of the Grant-Madsen model for combined wave–current bottom boundary layer flow originally written by Chris Sherwood. We thank Laura Landerman for conducting grain size and data analysis. This manuscript was improved by reviews by Dan Hanes, Pat Lynett, Eric Geist, and an anonymous reviewer. Discussion with Dave Rubin helped refine the conceptual model. The Tsunami Risk Assessment Project of the US Geological Survey Coastal and Marine Geology Program supported this research.

References

Bourgeois, J., Hansen, T.A, Wiberg, P.L., Kauffman, E.J., 1988. A tsunami deposit at the Cretaceous–Tertiary boundary in Texas. Science 241 (4865), 567–570.

Bourgeois, J., Petroff, C., Yeh, H., Titov, V., Synolakis, C.E., Benson, B., Kuroiwa, J., Lander, J., Norabuena, E., 1999. Geologic setting, field survey and modeling of the Chimbote, Northern Peru, tsunami of 21 February 1996. Pure and Applied Geophysics 154, 513–540.

Clague, J.J., Bobrowski, P.T., Hutchinson, I., 2000. A review of Geological records of large tsunamis at Vancouver Island, British Columbia, and implications for hazard. Quaternary Science Reviews 19, 849–863.

Corey, A.T., 1949. Influence of shape on the fall velocity of sand grains. MS thesis, Colorado A&M College, Fort Collins, Colorado.

Davies, H., 1999. Tsunami, PNG 1998. University of Papua New Guinea Press, Port Moresby. 49 pp.

Dawson, A.G., Long, D., Smith, D.E., 1988. The Storegga slides: evidence from eastern Scotland for a possible tsunami. Marine Geology 82, 272–276.

Dawson, A.G., Shi, S., Dawson, S., Takahashi, T., Shuto, N., 1996. Coastal sedimentation associated with the June 2nd and 3rd, 1994 tsunami in Rajegwesi, Java. Quaternary Science Reviews 15, 901–912.

Dietrich, W.E., 1982. Settling velocity of natural particles. Water Resources Research 18 (6), 1615–1626.

Drake, D.E., Cacchione, D.A., 1989. Estimates of suspended sediment reference concentration (Ca) and resuspension coefficient (γ_0) from near-bottom observations on the California shelf. Continental Shelf Research 9 (1), 51–64.

Gelfenbaum, G., Jaffe, B., 2003. Erosion and sedimentation from the 17 July, 1998 Papua New Guinea tsunami. Pure and Applied Geophysics 160, 1969–1999.

Gelfenbaum, G., Smith, J.D., 1986. Experimental evaluation of a generalized suspended sediment transport theory. In: Knight, R.J., McLean, J.R. (Eds.), Shelf Sands and Sandstones. Memoir, vol. 11. Canadian Society of Petroleum Geologists, pp. 133–144.

Goff, J.R., Rouse, H.L., Jones, S.L., Hayward, B.W., Cochran, U., McLea, W., Dickinson, W.W., Morley, M.S., 2000. Evidence for an earthquake and tsunami about 3100–3400 yr ago, and other catastrophic saltwater inundations recorded in a coastal lagoon, New Zealand. Marine Geology 170, 231–249.

Goff, J.R., McFadgen, B.G., Chague-Goff, C., 2004. Sedimentary differences between the 2002 Easter storm and the 15th-century Okoropunga tsunami, southeastern North Island, New Zealand. Marine Geology 204 (1–2), 235–250.

Hill, P.S., Nowell, A.R., Jumars, P.A., 1988. Flume evaluation of the relationship between suspended sediment concentration and excess boundary shear stress. Journal of Geophysical Research 93 (10), 12499–12509.

Hutchinson, I., Clague, J.C., Mathewes, R.W., 1997. Reconstructing the tsunami record on an emerging coast: a case study of Kanim Lake, Vancouver Island, British Columbia: Canada. Journal of Coastal Research 13 (2), 545–553.

Jaffe, B.E., Gelfenbaum, G., 2002. Using tsunami deposits to improve assessment of tsunami risk. Solutions to Coastal Disasters '02, Conference Proceedings. ASCE, pp. 836–847.

Jaffe, B., Gelfenbaum, G., Rubin, D., Peters, R., Anima, R., Swensson, M., Olcese, D., Bernales, L., Gomez, J., Riega, P., 2003. Tsunami deposits: identification and interpretation of tsunami deposits from the June 23, 2001 Peru tsunami. Proceedings of the International Conference on Coastal Sediments 2003, CD-ROM Published by World Scientific Publishing Corp and East Meets West Productions, Corpus Christi, TX, USA. ISBN: 981-238-422-7. 13 pp.

Kawata, Y., 1999. Field survey on the 1998 tsunami in northwestern area of Papua New Guinea. Report for Grant-Aid for Scientific Research (B)(1). Ministry of Education, Science, Sports and Culture, Japan. 81 pp.

Kawata, Y., Benson, B., Borrero, J., Davies, H., do Lange, W., Imamura, F., Letz, H., Nott, J., Synolakis, C.E., 1999. Tsunami in Papua New Guinea not as intense as first thought. Trans. Am. Geophys. U., vol. 80. EOS, pp. 101–105.

Kelsey, H.M., Nelson, A.R., Hemphill-Haley, E., Witter, R.C., 2005. Tsunami history of an Oregon coastal lake reveals a 4600 year record of great earthquakes on the Cascadia subduction zone. Geological Society of America Bulletin 117, 1009–1032.

Madsen, O.S., Chisholm, T.A., Wright, L.D., 1993. Suspended sediment suspension on the inner shelf during extreme storms. Proceedings of the 24th International Conference on Coastal Engineering. ASCE, vol. 2, pp. 1849–1864.

Meyer-Peter, E., Muller, R., 1948. Formulas for bed-load transport. Report on the Second Meeting of International Association for Hydraulic Research, pp. 39–64.

Minoura, K., Imamura, F., Takahashi, T., Shuto, N., 1997. Sequence of sedimentation processes caused by the 1992 Flores tsunami: evidence from Babi Island. Geology 25, 523–526.

Moore, A.L., 2000. Landward fining in onshore gravel as evidence for a late Pleistocene tsunami on Molokai, Hawaii. Geology 28 (3), 247–250.

Moore, A.L., Nishimura, Y., Gelfenbuam, G., Takanobu, K., Triv, R., 2006. Sedimentary deposits of the 26 December 2004 tsunami on the northwest coast of Aceh, Indonesia. Earth, Planets Space 58, 253–258.

Morton, R.A., Gelfenbaum, G., Jaffe, B.E., 2007. Physical criteria for distinguishing sandy tsunami and storm deposits using modern examples. Sed. Geology Special Issue 200, 185–208 (this issue).

Nanayama, F., Shigeno, K., Satake, K., Shimokawa, K., Koitabashi, S., Miyasaka, S., Ishii, M., 2000. Sedimentary differences between the 1993 Hokkaido-nansei-oki tsunami and the 1959 Miyakojima typhoon at Taisei, southwestern Hokkaido, northern Japan. Sedimentary Geology 135, 255–264.

Nanayama, F., Satake, K., Furukawa, R., Shimokawa, K., Atwater, B.F., Shigeno, K., Yamaki, S., 2003. Unusually large earthquakes inferred from tsunami deposits along the Kuril trench. Nature 424, 660–663.

Nilsen, P., 1992. Coastal bottom boundary layers and sediment transport. Advanced Series in Ocean Engineering 4 (324 pp.).

Nikuradse, J., 1933. Strömungsgesetze in rauhen Röhren, VDI Forschungsh., 361. (English translation, Laws of flows in rough pipes, NACA Tech. Memo. 1292, 62 p., Natl. Advis. Comm. For Aeron., Washington, D.C., 1950.)

Nishimura, Y., Miyaji, N., 1995. Tsunami deposits from the 1993 Southwest Hokkaido earthquake and the 1640 Hokkaido Komagatake eruption, Northern Japan. Pure and Applied Geophysics 144 (3/4), 719–733.

Panegina, T.K., Bourgeois, J., Bazanova, I.V., Braitseva, O.A., 2003. A millennial-scale record of Holocene tsunamis on the Kronotskiy Bay coast, Kamchatka, Russia. Quaternary Research 59, 26–47.

Peters, B., Jaffe, B., Gelfenbaum, G., Peterson, C., 2003. Cascadia tsunami deposit database: U.S. Geological Survey Open-File Report 03-13. 19 pp. plus electronic database and GIS coverage [URL: http://geopubs.wr.usgs.gov/open-file/of03-13/].

Peterson, C.D., Priest, G.R., 1995. Preliminary reconnaissance survey of Cascadia paleotsunami deposits in Yaquina Bay, Oregon. Oregon Geology 57 (2), 33–40.

Powers, M.C., 1953. A new roundness scale for sedimentary particles. Journal of Sedimentary Petrology 32, 117–119.

Sato, H., Shimamoto, T., Tsutsumi, A., Kawamoto, E., 1995. Onshore tsunami deposits caused by the 1993 Southwest Hokkaido and 1983 Japan Sea earthquakes. Pure and Applied Geophysics 144 (3/4), 693–717.

Shi, S., Dawson, A.G., Smith, D.E., 1995. Coastal sedimentation associated with the December 12th, 1992 tsunami in Flores, Indonesia. Pure and Applied Geophysics 144 (3/4), 525–536.

Smith, J.D., McLean, S.R., 1977. Spatially averaged flow over a wavy surface. Journal of Geophysical Research 82 (12), 1735–1745.

Titov, V.V., Synolakis, C.E., 1998. Numerical modeling of tidal wave runup. Journal of Waterway, Port, Coastal, and Ocean Engineering 124 (4), 157–171.

Titov, V.V., Jaffe, B.E., Gonzalez, F.I., Gelfenbaum, G., 2001. Re-Evaluating source mechanisms for the 1998 Papua New Guinea tsunami using revised slump estimates and sedimentation modeling. Proceedings of the International Tsunami Symposium, pp. 389–396.

Tuttle, M.P., Ruffman, A., Anderson, T., Jeter, H., 2004. Distinguishing tsunami and storm deposits in eastern North America: the 1929 Grand Banks tsunami versus the 1991 Halloween storm. Seismological Research Letters 75 (1), 117–131.

Vincent, C.E., Hanes, D.M., Bowen, A.J., 1991. Acoustic measurements of suspended sand on the shoreface and the control of concentration by bed roughness. Marine Geology 96, 1–18.

Walsh, T.J., Caruthers, C.G., Heinitz, A.C., Meyers III, E.P., Baptista, A.M., Erdakos, G.B., Kamphaus, R.A., 2000. Tsunami hazard map of the southern Washington coast: Modeled Tsunami Inundation from a Cascadia Subduction Zone Earthquake. Washington Division of Geology and Earth Resources, Geologic Map GM-49.

Wieberg, P.L., Rubin, D.M., 1989. Bed roughness produced by saltating sediment. Journal of Geophysical Research 94 (C4), 5011–5016.

Williams, H.F., Hutchinson, I., Nelson, A.R., 2005. Multiple sources for late-Holocene tsunamis at Discovery Bay, Washington State, USA. The Holocene 15 (1), 60–73.

Witter, R.C., Kelsey, H.M., Hemphill-Haley, E., 2001. Pacific storms, El Nino and tsunamis; competing mechanisms for sand deposition in a coastal marsh, Euchre Creek, Oregon. Journal of Coastal Research 17 (3), 563–583.

Yeh, H., Ghazali, A., Marton, I., 1989. Experimental study of bore runup. Journal of Fluid Mechanics 206, 563–578.